Preclinical Development of a Bispecific Antibody that Safely and Effectively Targets CD19 and CD47 for the Treatment of B-Cell Lymphoma and Leukemia

Vanessa Buatois, Zoë Johnson, Susana Salgado-Pires, Anne Papaioannou, Eric Hatterer, Xavier Chauchet, Françoise Richard, Leticia Barba, Bruno Daubeuf, Laura Cons, et al.

Preclinical development of a bispecific antibody that safely and effectively targets CD19 and CD47 for the treatment of B cell lymphoma and leukemia

Vanessa Buatois[1*], Zoë Johnson[1*§], Susana Salgado Pires[1], Anne Papaioannou[1], Eric Hatterer[1], Xavier Chauchet[1], Françoise Richard[1], Leticia Barba[1], Bruno Daubeuf[1], Laura Cons[1], Lucile Broyer[1], Matilde D'Asaro[2], Thomas Matthes[2], Simon LeGallou[3], Thierry Fest[3], Karin Tarte[3], Robert K. Clarke Hinojosa[4], Eulàlia Genescà Ferrer[4], José María Ribera[4], Aditi Dey[5], Katharine Bailey[5], Adele K. Fielding[5], Linda Eissenberg[6], Julie Ritchey[6], Michael Rettig[6], John F. DiPersio[6], Marie H. Kosco-Vilbois[1], Krzysztof Masternak[1], Nicolas Fischer[1], Limin Shang[1], and Walter G. Ferlin[1]

Affiliations.

[1] Novimmune S.A., 14, chemin des Aulx, 1228 Plan-les-Ouates, Switzerland

[2] Medical Faculty, University of Geneva, Rue Michel Servet, 1, 1211 Genève 4, Switzerland

[3] Rennes 1 University, Inserm U1236, 2, avenue du Pr Léon Bérard, 35043 Rennes, France

[4] Josep Carreras Leukaemia Research Institute (IJC), Campus ICO-Germans Trias Pujol, Ctra. de Can Ruti, Cami de les Escoles s/n, 08916, Badalona, Barcelona, Spain

[5] Paul O'Gorman Building, University College London (UCL) Cancer Institute, 72 Huntley Street, London, UK

[6] Washington University School of Medicine, Division of Oncology, Campus Box 8007, 660 South Euclid, St. Louis, MO 63110

[§] Current address: iOnctura SA, Avenue Sécheron 15, 1202 Geneva, Switzerland

* These authors contributed equally to this work.

Running title. Targeting CD47 in B cell malignancies

Corresponding author: Dr. Walter Ferlin, Novimmune S.A., 14 Chemin des Aulx, CH-1228 Plan-les-Ouates, Switzerland. Tel: +41 22 839 51 20; Fax: +41 22 593 71 41; E-mail: wferlin@novimmune.com

Conflict of interest. V.Buatois, Z.Johnson, S.Salgado Pires, A. Papaioannou, E.Hatterer, X.Chauchet, F.Richard, L.Barba, B.Daubeuf, L.Cons, L.Broyer, M.H.Kosco-Vilbois, K.Masternak, N.Fischer, L.Shang and W.G. Ferlin are current or former employees of Novimmune.

Abstract

CD47, a ubiquitously expressed innate immune checkpoint receptor that serves as a universal "don't eat me" signal of phagocytosis, is often up-regulated by hematological and solid cancers to evade immune surveillance. Development of CD47-targeted modalities is hindered by the ubiquitous expression of the target, often leading to rapid drug elimination and hemotoxicity including anemia. To overcome such liabilities, we have developed a fully human bispecific antibody, NI-1701, designed to co-engage CD47 and CD19 selectively on B cells. NI-1701 demonstrates favorable elimination kinetics with no deleterious effects seen on hematological parameters following single or multiple administrations to non-human primates. Potent *in vitro* and *in vivo* activity is induced by NI-1701 to kill cancer cells across a plethora of B cell malignancies and control tumor growth in xenograft mouse models. The mechanism affording maximal tumor growth inhibition by NI-1701 is dependent on the co-engagement of CD47/CD19 on B cells inducing potent antibody dependent cellular phagocytosis of the targeted cells. NI-1701-induced control of tumor growth in immunodeficient NOD/SCID mice was more effective than that achieved with the anti-CD20 targeted antibody, rituximab. Interestingly, a synergistic effect was seen when tumor-implanted mice were co-administered NI-1701 and rituximab leading to significantly improved tumor growth inhibition and regression in some animals. We describe herein, a novel bispecific antibody approach aimed at sensitizing B cells to become more readily phagocytosed and eliminated thus offering an alternative or adjunct therapeutic option to patients with B cell malignancies refractory/resistant to anti-CD20 targeted therapy.

Introduction

The incidence of hematological malignancies has been on the rise for the last 30 years, and accounts for approximately 9% of all cancers (1). Of the hematological malignancies, lymphoma is the most common type. B cell lymphomas are far more frequent than T-cell lymphomas accounting for around 85% of all Non-Hodgkin lymphomas (NHL). The introduction of rituximab, the first anti-CD20 monoclonal antibody (mAb), has revolutionized the management of B cell lymphomas (2). Rituximab plus the "CHOP" (i.e., cyclophosphamide, doxorubicin, vincristine, and prednisone) chemotherapy regime is the frontline treatment for B cell lymphomas (3). However, 30-60% of indolent NHL patients are resistant to rituximab at baseline and up to 50% of patients suffer relapses after anti-CD20 therapies and become refractory to their treatment (4).

Two major mechanisms underlying rituximab relapse/refractory responses are low CD20 expression levels in some lymphoma patients and downregulation of CD20 expression post anti-CD20 treatment (5, 6). CD19, a B cell specific marker, has been considered to be a promising target to overcome the anti-CD20 resistant/refractory situation. CD19 is a transmembrane glycoprotein of the immunoglobulin (Ig) superfamily. It is expressed during different stages of B cell development, starting from pre-B cell stage till being down-regulated in early plasma cells (7). Furthermore, CD19 is broadly expressed in B cell malignancies including those which are CD20 positive (e.g., NHL and B-chronic lymphocytic leukemia (B-CLL)) and those which may be CD20 low or negative (e.g., B-acute lymphoblastic leukemia (B-ALL)) (8). Consistent with its broad expression spectrum in B cell malignancies, targeting CD19 with different strategies (e.g., CD3/CD19 bispecific, CD19 CAR T cells) to harness B cell killing has generated promising results in several clinical trials (9-11).

The emergence of "checkpoint inhibitors", e.g., antibodies that block the interaction of PD-1 with its ligand PD-L1, thereby unleashing the natural brake on T-cells and boosting the immune response represent a paradigm shift in our approach to treating cancer (12). In addition to harnessing the adaptive immune response to fight malignant cells, attention has turned to the innate immune system, in particular macrophages, a cell population which is abundant in the tumor microenvironment and which plays a specific role in phagocytosing cancer cells (13).

Macrophages express signal regulatory protein α (SIRPα) that interacts with CD47, a ubiquitously expressed protein that mediates a "don't eat me" signal. Cancer cells have evolved to hijack this interaction by upregulating the expression of CD47 on their cell surface, thus counterbalancing prophagocytic signals and increasing the chance of evading innate immune surveillance (14).

Therefore, blockade of the CD47/SIRPα interaction represents a promising strategy to increase the phagocytic clearance of tumor cells from the body. Several mAb and fusion proteins that target this interaction are in early clinical development (clinicaltrials.gov; e.g. NCT02953509, NCT03013218, NCT02367196 and NCT02890368). One limitation of this approach is that CD47, whilst upregulated on tumor cells (15), is also ubiquitously expressed on all cells of the body, including relatively high levels on erythrocytes and platelets (16, 17). Monospecific agents targeting CD47 would thus be expected to exhibit poor pharmacokinetic properties due to target mediated drug disposition (TMDD) and possible side effects including anemia.

We have recently described a fully human bispecific antibody (biAb) format, the κλ-body (18). Using this format, we generated a panel of biAb comprising a high affinity CD19 targeting arm combined with CD47 blocking arms with a range of affinities, on a human IgG1 Fc backbone to impart full effector mechanisms (19). The resultant biAbs are able to selectively block the interaction CD47/SIRPα on $CD19^+$ cells and induce tumor cell killing *in vitro* and *in vivo*. From the panel of biAbs, we selected the CD47 arm with the appropriate affinity needed to balance efficacy on $CD19^+$ cells against "off-target" effects, i.e., an affinity that is weak enough to result in a fast off-rate for CD47 on non $CD19^+$ cells.

Here we describe the preclinical characterization of NI-1701, which induces potent macrophage-mediated phagocytosis of tumor cell lines and primary samples representing various B cell malignancies. We also present *in vivo* proof of efficacy data using several mouse models. Together with non-human primate studies, these data suggest that NI-1701 may be an effective and safe anti-cancer therapeutic both as a monotherapy and in combination.

MATERIAL AND METHODS

Cell lines and primary samples

The Burkitt's lymphoma Raji (CCL-86) and Ramos (CRL-1596) cell lines, the B-ALL NALM-6 (ACC-128), and the DLBCL SUDHL-4 (CRL-2957) cell lines were obtained from the ATCC. B-CLL MEC-2 cell line (ACC 500) was obtained from DMSZ. Cells were obtained between 2010 and 2014, authenticated and mycoplasma tested by the suppliers. Cell lines have been retested internally before the experiments. After thawing, cells were cultured between two weeks and two months. The Raji CD47 silenced cell line was derived from original wild-type (wt) Raji cells transfected with short hairpin (sh) RNA, subcloned, screened by flow cytometry and finally selected as the most silenced stable clone by quantification of CD47 receptors using QIFIKIT® (DAKO). Cells were cultured at 37°C and 5% CO2. Primary samples were collected from Conversant Biologics (Huntsville, USA), the Leukemia Research Center (Glasgow, UK), the Geneva University Hospital (Geneva, Switzerland), the Josep Carreras Leukaemia Research Institute (Barcelona, Spain) and the CeVi collection of the Institute Carnot/CALYM (ANR, Rennes1 University, France). The ethics approvals were obtained from appropriate research ethics committees. Samples were obtained in agreement with the principles of the Declaration of Helsinki. Each patient provided and signed a written informed consent. The study was approved by the Institutional Review Board of the different collaborating hospitals.

Reagents

NI-1701, CD47 monovalent Ab, CD19 monovalent Ab, and CD19/CD47^{hi} biAb were generated using a fixed Ig heavy chain variable domain (VH) library construction and produced as described in detail by Fischer et al. (18). Human (h) IgG1 isotype-matched control mAb was produced and purified at Novimmune from Chinese Hamster Ovary (CHO) culture supernatants. The CD19 monovalent Ab contains the same anti-CD19 arm as NI-1701 and an irrelevant nonbinding arm, while the CD47 monovalent Ab contains the same anti-CD47 arm as NI-1701 and an irrelevant nonbinding arm. The bivalent CD19 Ab (i.e., a mAb) contains the same anti-CD19 arm as NI-1701. The CD19/CD47^{hi} biAb contains the same anti-CD19 arm as NI-1701 and an anti-CD47 arm with a higher affinity than NI-1701 for CD47. Clinical-grade rituximab (anti-CD20 hIgG1 mAb) was obtained from FarmaMondo. The neutralizing anti-hCD47 mAb mouse B6H12 was cloned and expressed as hIgG1 in CHO cells (hB6H12). The anti-CD47 mAb, 5F9 (20), was cloned and expressed as hIgG4 in CHO cells.

Quantification of cell surface receptor density

Receptor density was quantified following manufacturer's instruction (QIFIKIT®, Dako). Briefly, following incubation with Fc Receptor (FcR) Blocking reagent (Miltenyi Biotec, cat # 130-059-901), primary Abs (50 µg/mL) anti-hCD19 (BD Biosciences, cat # 555410), -hCD47 (eBiosciences, cat # 11-0478-42) and -hCD20 (R&D Systems, cat # MAB4225) were added to the samples (whole blood or cells) for 30 min at 4°C. 100 µL of Calibration beads were washed along with the cells and treated identically. 100 µL of secondary Ab (1/50 in PBS BSA 2 %) were added for 30 min at 4°C. Cells were washed and resuspended in 130 µL of CellFix (Becton Dickinson (BD) Biosciences) and acquired on FACS Calibur (BD Biosciences). Analysis was performed and Mean Fuorescence Intensity (MFI) was determined. A linear regression was performed using MFI values from the calibration beads. Receptor density per cell was extrapolated from this regression line.

Whole blood binding

Human whole blood samples were collected from healthy donors in citrate at the Blood Transfusion Center in Geneva. Samples were mixed with 3 µg/mL of AF488-coupled NI-1701, hB6H12 or isotype control (using the Alexa Fluor 488 Protein Labeling Kit (A10235, Thermo Fisher Scientific)) and surface staining Abs for 30 min at 4°C. More precisely, samples were incubated with PE anti-hCD41a (#555467, BD Biosciences), APC-Cy7 anti-hCD3 (#557757, BD Biosciences) and with BV510 anti-hCD20 (#302311, BioLegend) Abs. Whole blood was then divided in two samples: 5 µL were diluted in PBS for erythrocytes analysis while 150 µL were incubated with erythrocyte lysing solution (#349202, BD Biosciences), and washed for leukocytes and platelets analysis. Samples were then acquired on a CytoFLEX instrument (Beckman Coulter) and analyzed with Flowjo® software.

Affinity measurements

The affinity (K_D) for the binding to CD19 was determined on a 3200 KinExA (Sapidyne) while the binding to CD47 was determined using Surface Plasmon Resonance (SPR) on a Biacore T200 instrument (GenScript). The affinity for CD19 was determined on $CD19^+$ Raji B cells with a F(ab')2 of the CD19 arm, while the affinity for CD47 was determined using recombinant hCD47 protein with NI-1701.

Antibody Dependent Cellular Phagocytosis

Human peripheral blood mononuclear cells (PBMCs) were isolated from buffy coats by Ficoll gradient. Classical macrophages (M0) were prepared as previously described (19). M1 macrophages were generated from PBMCs with 20 ng/mL recombinant hMCSF for 14 days with the addition of 50 ng/mL of hIFNγ during the last 18h of culture. For M2a or M2c polarization, macrophages were generated from PBMCs supplemented with 20 ng/mL recombinant hMCSF for 14 days with the addition of either 20 ng/mL of hIL-4 or 10 ng/mL of hIL-10 + 20 ng/mL of hTGFβ during the last 18h of culture, respectively (21-23). Target cells stained with 0.2 µM CFSE (Invitrogen) were opsonized with the tested Abs for 15 min at 37°C. The flow cytometry based phagocytosis assay used is described elsewhere (19). In here, the ratio between effector (macrophages) and target cells was 1:5. The percentage of phagocytosis is defined as the percentage of macrophages having engulfed at least one target cell and identified as $CD14^+$ $CFSE^+$ double-positive events amongst the total live $CD14^+$ macrophages. In some experiments, the FlowSight® imaging flow cytometer was used to investigate the phagocytosis index defined as the number of target cells engulfed per 100 macrophages. Fluorescence microscopy was also used. Here, monocytes were isolated from healthy donor buffy coats using the Human Pan Monocyte Isolation Kit (Miltenyi Biotec). 15,000 monocytes were plated in 16-well chamber slide, in 100 µl of RPMI/10% heat inactivated FCS with 50 ng/mL hM-CSF + (h-IL4 and h-IL10) (20 ng/mL each) to obtain M2 macrophages. At day 10, M2 macrophages were washed and stained with 0.2 µM CFSE. The day of the phagocytosis assay, B cells from lymph node biopsies were purified using the Human B cell Isolation Kit II (Miltenyi Biotec). Purified B cells were stained with 60 ng/mL of pHrodo solution (#P36600, ThermoFischer, 12 min, RT) opsonized with 10 µg/mL of NI-1701, rituximab or hIgG1 isotype control Ab. Cells were then added on macrophages to obtain the final 1:5 ratio between effector and target cells. Cells were cocultured in chamber wells (3h, 37°C) and analyzed by fluorescence microscopy using FIJI software. The percentage of phagocytosis is defined as the percentage of macrophages that have engulfed at least one target cell and identified as $pHRodo^+$ $CFSE^+$ double-positive events amongst 100 counted macrophages.

Antibody Dependent Cellular Cytotoxicity

1-2 $x10^6$ cells/mL healthy PBMC were activated overnight at 37°C with RPMI/10% heat inactivated FCS supplemented with 10 ng/mL of recombinant hIL-2. The next day, 5000 Raji cells were incubated with 100 µCi Cr51 (Perkin Elmer, 37°C, 1h). After washing, cells were opsonized with NI-1701 or hIgG1 control (30 min, 37°C). 5,000 Cr51-loaded Raji cells were then mixed with 400,000

PBMC cells to obtain the final 80:1 ratio between effector (PBMC) and target cells (Raji cells). The cell mixture was incubated for 4h at 37°C before being centrifuged for 10 min at 1500 rpm. Supernatant was transferred into a LumaPlate (coated with scintillant) and counted in a γ-counter. Negative controls (spontaneous Cr51 release) consisted of Cr51-loaded target cells incubated with medium in the absence of effector cells. Total lysis control consisted of Cr51-loaded target cells incubated with 5 µL of cell lysis solution (Triton X-100). Nonspecific lysis control (baseline) consisted of Cr51-loaded target cells incubated with effector cells, without Ab. The ADCC percentage was calculated using the following formula: % specific ADCC = ((sample counts per minute (cpm) – nonspecific lysis control cpm)/(total lysis control cpm – negative control cpm)) x 100%.

Cell-derived xenograft model in mice

In accordance with the Swiss animal protection law, 5 x 10^6 Raji cells were injected subcutaneously into the flank of 6- to 10-week-old NOD/SCID mice (Charles River Laboratories). Tumor volume was measured using a caliper and calculated using the formula (width x length x height) x π/6. Mice received 4 or 5 doses of 10mg/kg or 20mg/kg of Abs by intravenous (i.v.) administration (tail vein) once a week during 4 or 5 weeks. Mice were euthanized when the set endpoint of the experiment was reached (tumor volume≈1400mm^3) or at the end of the study. Percentage of tumor growth inhibition, in comparison to hIgG1 control group was determined using the formula: %TGI = {1- [(T_t–T_0)/(V_t-V_0)]} x 100, where T_t = mean tumor volume of treated at time t, T_0 = mean tumor volume of treated at time 0, V_t = mean tumor volume of control at time t and V_0 = mean tumor volume of control at time 0. Survival time is the time between the initiation of the treatment to the euthanasia of the mice when the set endpoint of the experiment was reached (tumor volume≈1400mm^3).

Patient-derived xenograft model in mice

This experiment was performed in accordance with the United States animal protection law and Institutional animal guidelines. NSG mice irradiated 2 days earlier (275cGy) were injected i.v. with 1.8x 10^6 PBMC from an ALL patient (invaded with 90% of cancer cells). Mice were i.v. treated with hIg1 control or NI-1701 Abs (20 mg/kg) at days 7, 14, 21, 28 and 35. Upon sacrifice, peripheral blood (PB), spleen, liver and bone marrow (BM) were harvested and subjected to flow cytometry to detect the human ALL cells identified as $hCD45^+$, $hCD3^-$, $hCD14^-$ $hCD56^-$ using fluorescent labeled Abs.

Pharmacokinetics and Dose Range Finding studies in cynomolgus monkeys

A single-dose (SD) pharmacokinetics (PK) study and a dose range finding study (DRF) were performed in cynomolgus monkeys at Covance Laboratories test facilities. All procedures in the studies were in compliance with the German Animal Welfare Act or the UK Animals (Scientific Procedures) Act 1986 and were approved by the local Institutional Animal Care and Use Committee. For the SD study, 2- to 3-year-old females (n = 3/dose group) were injected by i.v. bolus with either 0.5 mg/kg or 10 mg/kg of NI-1701 or CD19/CD47^{hi} biAb. For the DRF study, one male and two females of 2- to 3-year-old received weekly i.v. bolus injections of NI-1701 or vehicle for 4 weeks. The NI-1701-treated animals received two injections at 30 mg/kg (Days 1 and 8) followed by two injections at 100 mg/kg (Days 15 and 22). Control group animals received i.v. bolus injections of vehicle only on days 1, 8, 15 and 22. For both studies, the animals were assessed twice daily for clinical signs and blood samples collected at different time points for hematological and PK analyses. NI-1701 and CD19/CD47^{hi} biAb serum concentrations were measured by ELISA at Novimmune with in-house developed assay. IL-6 serum concentrations were measured using MILLIPLEX MAP multiplex immunodetection kits (Millipore) and analysed on the Luminex® instrument. The evaluation of the PK data was conducted at Novimmune using WinNonlin software (Professional Version 6.3, Pharsight).

Statistical Analysis

GraphPad Prism 6 was used for all statistical analysis depicted in each figure legend. Data are expressed as mean ± SEM or mean ± SD, as indicated.

RESULTS

The anti-CD19/CD47 biAb, NI-1701, specifically binds to B cells in whole blood

As CD47 is a ubiquitously expressed molecule (24, 25), we designed a biAb, NI-1701, that consists of a CD47 binding arm with an affinity that affords rapid engagement/disengagement kinetics when binding CD47 in a monovalent setting. This arm is paired with a high affinity CD19 binding arm, in a fully human biAb, the κλ-body (18). More precisely, the affinity to CD19 was measured to be subnanomolar (i.e. 0.6nM) while the affinity to CD47 is 500 nM. In order to assess the specificity of NI-1701, the binding profile to B cells was assessed in whole blood using flow cytometry. While CD47 is expressed on various cells in whole blood, including T cells, platelets and erythrocytes (Supplementary Table S1), NI-1701 substantially shifted the signal for binding only to the B cells and rather weakly if at all to platelets, T cells and erythrocytes as compared to the irrelevant isotype control (Fig. 1). Conversely, the CD47 mAb, hB6H12, used as a control for CD47 expression, significantly bound to all cell populations (Fig. 1).

The specific blockade of CD47/SIRPα interaction on CD19 expressing cells mediates potent macrophage-dependent phagocytosis of the target cells

Having demonstrated the specific binding of NI-1701 to B cells, we then assessed the *in vitro* efficacy of this compound to mediate phagocytosis of $CD19^+$ B cells by macrophages. For this, CFSE-labeled Raji cells (Burkitt lymphoma) were used as target cells in an antibody dependent cellular phagocytosis (ADCP) assay using hM-CSF differentiated macrophages as effector cells. The results demonstrated a dose dependent phagocytosis of Raji cells mediated by NI-1701, with an EC_{50} of 7.44 ng/mL (Fig. 2A) and a maximum of 42% of phagocytic macrophages. Furthermore, using video microscopy to view phagocytosis in real-time, we observed that these phagocytic macrophages sequentially engulfed not only one but several tumor target cells in response to NI-1701 treatment (Supplementary Video S1). In contrast, in the presence of a hIgG1 isotype control, no phagocytic activity was observed (Supplementary Video S2).

To demonstrate the requirement of the co-engagement of both targets by NI-1701 to reach the maximal potency, NI-1701-mediated phagocytosis was compared to control monovalent variants. The CD47 monovalent variant contains only the anti-CD47 binding arm of NI-1701 (CD47 monovalent Ab) while the CD19 monovalent variant contains the anti-CD19 binding arm of NI-1701 (CD19 monovalent Ab) combined to an irrelevant arm. The control monovalent Abs elicited a weaker

potency of phagocytosis as compared to NI-1701, with a 4.2-fold decrease for the CD19 monovalent Ab (EC_{50} of 31.11 ng/mL) and a 52-fold decrease for the CD47 monovalent Ab (EC_{50} of 385.3 ng/mL) (Fig. 2A). Interestingly, the bivalent CD19 Ab (containing the same anti-CD19 arm as NI-1701) induces similar potency to NI-1701 (i.e., EC_{50} at 7.7 ng/mL), although less effective at inducing maximum phagocytosis (Fig.2A).

In order to demonstrate the contribution of CD47/SIRPα interaction to phagocytosis, we generated Raji cells with a minimal expression level of CD47, while the levels of CD19 and CD20 remain unchanged (Fig. 2B). We then assessed the activity of rituximab on the wt versus the CD47 silenced Raji cells. While rituximab mediated efficient phagocytosis of the wt Raji cells, the knockdown of CD47 on the target cell surface results in an enhanced potency of rituximab by 5 fold (Fig. 2C), demonstrating that the reduction of the CD47/SIRPα interaction enhances CD20 mediated targeted cell killing. A similar result was seen with the CD19 monovalent Ab, in that silencing of CD47 enhanced Ab mediated phagocytosis. In contrast, and as expected, NI-1701 demonstrated a similar potency on both cell populations which was equal to the efficacy of the anti-CD19 monovalent Ab killing of CD47 silenced Raji cells (Fig. 2D).

Next, the ability of NI-1701 and rituximab to mediate phagocytosis was compared using human $CD19^+/CD20^+$ cancer cell lines derived from patients with Non-Hodgkin lymphoma (NHL; Raji and Ramos), ALL (NALM-6), CLL (MEC-2) or DLBCL (SUDHL-4). NI-1701 was as potent as rituximab at mediating phagocytosis of the Raji, Ramos and MEC-2 cell lines (Fig. 3A). NALM-6 cells, which express a low level of CD20 (Supplementary Table S2), were weakly phagocytosed in the presence of rituximab whereas NI-1701 mediated a potent effect (Fig. 3A). SUDHL-4 cells were efficiently phagocytosed by both NI-1701 and rituximab, although the anti-CD20 mAb was slightly more effective (Fig. 3A), which may be explained by the high level of CD20 (Supplementary Table S2).

Using *in vitro* polarized macrophages to mimic the situation of the tumor microenvironment, the ability of NI-1701 to engage different subtypes of macrophages to mediate phagocytosis of cancer target cells was assessed. Classical M-CSF cultured macrophages (M0), M1 macrophages polarized using IFNγ as well as M2 phenotypes, defined as M2a and M2c, generated by the addition of IL-4 or IL-10 + TGFβ, respectively, were used. NI-1701 mediated a similar level of phagocytosis of Raji cells by all subsets of macrophages with up to 40 to 50% of the macrophages being phagocytic (Fig. 3B). A 5.4, 4.3, 4.7 or 4.2 fold increase in phagocytosis by NI-1701 opsonized-Raji cells was observed as compared to the isotype control for the *in vitro* macrophages polarized into M0, M1, M2a or M2c subtypes, respectively (Fig. 3B).

Finally, as a fully human IgG1 Ab, we wanted to investigate whether NI-1701 was able to mediate other Fc-dependent effector mechanisms such as antibody-dependent cellular cytotoxicity (ADCC). As expected, a dose-dependent killing by ADCC of Raji cells in the presence of NI-1701 was observed (Fig. 3C).

NI-1701 controls tumor growth *in vivo*

We next sought to assess the *in vivo* anti-tumor killing efficacy of NI-1701 in a mouse xenograft model using NOD/SCID mice implanted with Raji cells. NI-1701 was significantly efficacious in controlling tumor growth, with a final tumor growth inhibition (TGI) of 79% as compared to the control (Fig. 4A, upper panel). The monovalent variants of NI-1701, i.e., CD47 and CD19 monovalent Abs, showed a partial effect on tumor growth with a final TGI of 54% and 46%, respectively. The bivalent CD19 Ab only demonstrated a partial effect with a final TGI of 36%. Tumor growth was monitored beyond the end of the treatment period demonstrating that NI-1701 affords a longer period of slowing tumor growth compared with both monovalent Abs and the bivalent CD19 Ab (Fig. 4A, lower panel). These results confirmed that co-engaging both CD47 and CD19 by NI-1701 promotes a more potent antitumor effect.

Next, the activity of NI-1701 was compared to the anti-CD20 mAb, rituximab. Since combination therapies are widely used in oncology clinical practice we tested the hypothesis that targeting two different B cell epitopes in conjunction with blockade of the CD47/SIRPα interaction may lead to enhanced tumor control. As expected, rituximab significantly reduced tumor growth compared to hIgG1 control treated group (Fig. 4B, upper panel). Interestingly, NI-1701 was superior to rituximab at reducing tumor growth (72% vs 48% of TGI for NI-1701 and rituximab, respectively). Finally, the combination therapy of NI-1701 and rituximab led to higher inhibition (92%) of tumor growth until the end of the treatment period at day 26. Tumor growth was monitored beyond the end of the treatment period and the data demonstrate that NI-1701 affords a longer period of slowing tumor growth than rituximab, and that the combination of the two resulted in a 2.45-fold increase in the survival time from a median of 24.5 days for isotype control treated animals to 60 days for the combination therapy treated group (Fig. 4B, lower panel).

NI-1701 demonstrates a favorable pharmacokinetic and safety profile in nonhuman primates

To evaluate PK and safety parameters, NI-1701 was administered to cynomolgus monkeys. The anti-CD19 arm of NI-1701 is not cross-reactive to cynomolgus monkey while the CD47 arm has a similar binding profile for cynomolgus monkey and human CD47. This allowed us to test the hypothesis that the affinity for CD47 was sufficiently low to circumvent potential liabilities of targeting the ubiquitously expressed CD47, i.e. rapid drug elimination kinetics through TMDD and target related toxicity including anemia. NI-1701 was administered once as an i.v. bolus, at a high (10 mg/kg) or low (0.5 mg/kg) dose, and serum concentrations of the compound were measured. The terminal elimination profile of NI-1701 was parallel for both doses, suggesting that no target mediated mechanisms contributed to the clearance of the biAb (Fig. 5A). Furthermore, the PK parameter estimates for NI-1701, i.e., half-life and clearance, were 110h and 12.24 mL/day/kg, close to those of other hIgG1 molecules that have been reported during preclinical and clinical development (26).

In order to evaluate the impact that a higher affinity binding to CD47 may have on Ab clearance, we compared the PK of NI-1701 with another bispecific molecule having the same (non-cross reactive) CD19 targeting arm but a CD47 blocking arm with a higher affinity (i.e., 100 nM), noted as CD19/CD47^{hi} biAb. NI-1701 and CD19/CD47^{hi} biAb have similar functional potency (Supplementary Figure S1). The PK profile of the latter has been described elsewhere (19). The two biAbs have similar half-lives (110h for NI-1701 and 106h for CD19/CD47^{hi} biAb) but the clearance parameters are different, with the CD19/CD47^{hi} biAb exhibiting a high clearance value (i.e., 18.24 mL/day/kg) as compared to 12.24 mL/day/kg for NI-1701. Examination of the distribution phase (i.e., alpha phase) of NI-1701 versus the CD19/CD47^{hi} biAb during the first 24 hours following i.v. bolus revealed that, at both high and low doses, the initial serum concentration measurements for NI-1701 were higher than for CD19/CD47^{hi} biAb (Fig. 5B). This result suggests an early binding event which impacts the distribution phase and results in a higher clearance for the higher affinity CD47 binding molecule. The ratio of $AUC_{0\text{-}inf}$ shows that an even greater proportion of CD19/CD47 ^{hi} biAb is undetected at the low dose versus the high dose compared with NI-1701 (59% at 0.5 mg/kg compared with 67% at 10 mg/kg), suggesting that a target mediated event occurs (Supplementary Table S3). Finally, while no hematological toxicity was observed, an increase in circulating IL-6 levels following CD19/CD47^{hi} biAb injection was detected (Fig. 5C).

A DRF study was conducted with NI-1701 in cynomolgus monkeys where treated animals received 2 i.v. bolus injections at 30 mg/kg at weeks 1 and 2, followed by two injections at 100 mg/kg at weeks 3 and 4. The mean Cmax values on weeks 1 and 3 (post the first dose at 30 and the first dose at

100mg/kg, respectively) were 1003.47 and 3149.36 µg/mL, respectively, showing dose proportionality with the single dose study (Supplementary Table S4). Furthermore, a minimal accumulation of NI-1701 was seen between the first and second injection at each dose level (Fig. 5D). No signs of anemia or thrombocytopenia were observed as red blood cell and platelet levels remained within normal ranges throughout the study (Fig. 5E). There were no drug related observations. NI-1701 was well tolerated at doses up to 100 mg/kg. Complete haematological results from the study are tabulated in Supplementary Table S5. Further *in vitro* safety assessments were performed on human and/or cynomolgus whole blood to assess hemaglutination and platelet aggregation, and no findings related to NI-1701 were observed whereas anti-CD47 mAbs showed effects on both parameters (Supplementary Figure S2A, B, C and D).

NI-1701 effectively kills primary leukemia and lymphoma cells

In order to demonstrate the clinical relevance of targeting CD47 on $CD19^+$ cancer cells, the *in vitro* studies were extended to primary cells obtained from patients with B cell leukemias or lymphomas. NI-1701 mediated an efficient and potent phagocytosis of primary cells from 24 individual CLL patients (Fig. 6A). Imaging confirmed the engulfment of the target cells by visualizing the double labeling of the $CD14^+$ phagocytes and the $CFSE^+$ target cells (Fig. 6B, left panel). Calculating the phagocytic index revealed that a mean of 175 (+/- 80) B-CLL cells opsonized with NI-1701 were phagocytized by every 100 macrophages (Fig. 6B, right panel). Similar results were obtained with rituximab (Fig. 6A and Fig. 6B).

Cells from bone marrow aspirates of 12 and whole blood of 3 patients with B-ALL, a leukemia with limited treatment options, were also obtained and used in the ADCP assay. A significantly enhanced phagocytosis of target cells in the presence of NI-1701 was consistently observed with a maximum percentage of phagocytosis ranging from 46.4 to 86.3% and a mean value of 62.5% (+/- 13.6). The activity of NI-1701 was three times higher than the isotype control and significantly higher than rituximab (43.26% +/- 19.1) (Fig. 6A). NI-1701 induced phagocytosis was also tested using samples from 13 cancer patients diagnosed with different subtypes of NHL including the following cases: 3 marginal zone lymphomas (MZL), 2 Waldenstrom macroglobulinemias (WM), 3 mantle cell lymphomas (MCL), 4 follicular lymphomas (FL) and 1 DLBCL. A significantly higher and similar phagocytosis was induced following NI-1701 or rituximab treatment as compared to the control IgG1, with maximum percentage ranging from 58.3 to 97.9% and from 55.3 to 98.5%, respectively (Fig. 6A). To further investigate the capacity of NI-1701 to mediate phagocytosis of NHL tumor cells,

purified B cells isolated from lymph node biopsies of 10 FL patients were used as target cells. NI-1701 and rituximab induced equivalent phagocytosis of these patients' FL B cells (Fig. 6C).

Using a patient cell derived model (PDX) generated with PBMCs from a B-ALL patient, the ability of NI-1701 to kill primary tumor cells *in vivo* was evaluated. Mice were i.v. injected with patient-derived B-ALL cells, and 7 days later treated either with NI-1701 or isotype control Ab. Analysis of the bone marrow, peripheral blood, spleen and liver demonstrated that, while B-ALL cells were present in these compartments following hIgG1 control Ab treatment, NI-1701 eradicated the tumor burden (Fig. 6D).

Discussion

Approaches targeting CD47 face considerable development challenges due to the ubiquitous expression pattern of the target on healthy cells. As such, hematotoxicity and poor pharmacokinetics are common unwanted secondary effects that have been described in studies conducted in mice and non-human primates (20, 27-30). The primary differentiating characteristic of the biAb approach is its increased selectivity for the target, i.e., $CD19^+$ B cells. While CD47 is expressed on all cell types in whole blood, including T cells, platelets and erythrocytes, flow cytometry analysis demonstrates that NI-1701 binds strongly to human B cells with no detectable binding to T cells and erythrocytes and weak binding to platelets. The lack of detectable binding to erythrocytes is consistent with the lack of hemagglutination seen in the presence of NI-1701. The weak NI-1701 binding activity on platelets is most probably due to the co-engagement of the Fc-portion of the biAb interacting with the low-affinity FcγRIIA (31) and the low-affinity CD47 arm on the same cell. This binding event has no functional consequence, such as platelet aggregation or activation *in vitro*. Furthermore, single or multiple doses of NI-1701 in non-human primates are well tolerated, demonstrating favorable pharmacokinetic profiles with proportionality between the doses and, importantly, no hematological toxicity. Disrupting the CD47/SIRPα axis with the "right" affinity CD47-binding arm is key to the biAb approach. Indeed, in the process of selecting a lead candidate for preclinical development, a higher affinity CD47-binding arm was tested in the biAb format (i.e., CD47/CD19) and administered to NHP. Interestingly, while no hematological toxicity was observed, the higher CD47 binding resulted in rapid decrease in initial plasma concentration (alpha phase). We hypothesize that this drop in the alpha phase concentration is due to a binding event in blood leading to a faster clearance, which is supported by our *in vitro* observation in whole blood demonstrating increased binding to erythrocytes and platelets. Furthermore, these data corroborate previous published results of a biAb with reduced affinity for CD47 which allows for selective binding to dual antigen-expressing cells in the presence of a large CD47-sink (32). Finally, the lower affinity CD47-binding arm of NI-1701 was far less prone to inducing cytokine release *in vitro* as compared to the CD19/$CD47^{hi}$ BiAb. Taken together, the selectivity afforded by the high affinity CD19-binding arm coupled to a low affinity CD47-binding arm has the potential to significantly widen the safety margin of therapeutic CD47 targeting in patients.

Therapeutic Abs targeting B cells exert antitumor activities through various Fc-mediated mechanisms including ADCP and ADCC. These attributes have been extensively described pre-clinically as key mechanisms in the elimination of cancer B cells by anti-CD20 (33) and anti-CD19 Abs (34, 35). However, to avoid indiscriminate elimination of healthy host cells by CD47-targeting

mAbs through Fc-mediated effector functions, the Fc domains of the anti-CD47 mAbs have been selected for reduced effector functions, e.g. IgG4 (20). This limits the tumor-killing capacity of the anti-CD47 mAbs as a monotherapy. In contrast, due to its selective targeting to $CD19^+$ cells, NI-1701 is a fully hIgG1 with the whole spectrum of Fc-mediated effector function. We show here that NI-1701 mediates effective killing of primary and immortalized cancer cells via ADCP and ADCC. The ability for NI-1701 to harness the anti-tumor potency of the tumor infiltrating myeloid cells through blockade of CD47/SIRPα interaction was demonstrated via effective *in vitro* phagocytosis of cancer cells taken from a plethora of B-cell malignancies. In addition, NK cells were shown to be efficient killers by ADCC of malignant B cells in the presence of NI-1701, in line with several reports demonstrating the importance of these cells for the cytotoxic activity of several mAbs (36-38).

We extended our *in vitro* findings to demonstrating efficacy induced by co-targeting CD47/CD19 *in vivo*. NI-1701 administration to Raji B cell-transplanted NOD/SCID mice resulted in control of tumour growth and a significant increase in median survival time as compared to isotype control treated mice. Co-engagement of CD47/CD19 is obligate for maximal efficacy as the CD19 monovalent biAb, the CD47 monovalent biAb and the bivalent CD19 allow only for partial control of tumor growth. Interestingly, the monovalent CD47 Ab showed equivalent activity to the CD19 monovalent Ab *in vivo*. This result was not predicted by the *in vitro* killing data, where the latter was more potent. Nonetheless, the *in vivo* observation is explained by the high dose of CD47 monovalent Ab given to mice allowing exposure levels to reach Ab concentrations known to induce maximal ADCP activity *in vitro*. The potent *in vivo* anti-tumor effect of NI-1701 was also demonstrated in a patient-derived xenograft model of B-ALL in which NI-1701 reduced tumor across the various organs tested. Studies are underway to dissect underlying mechanism. Nonetheless, the data herein derived from xenograft experiments in NOD/SCID or NSG mice, characterized by impaired T/B development, reduced NK cell function (39, 40) and the ability for mSIRPα to bind hCD47 with high affinity (41), suggest that macrophages will be the main driver for the observed tumor control *in vivo*. Tumor-associated macrophages (TAMs), displaying diverse phenotypes (42), represent key regulators of the complex interplay between the immune system and cancer in humans and mice (43, 44) and consequently efforts are focusing on targeting TAMs in oncology (Reviewed in (45)). In general, M2-macrophages which exert anti-inflammatory and pro-tumorigenic activities, are described to support tumor growth as opposed to the M1-macrophages understood to induce inflammatory responses (43, 46). Our *in vitro* analysis demonstrated that monocyte-derived M1 and M2-macrophages effectively kill Raji B cells in the presence of NI-1701. The results suggest that NI-1701 may re-educate M2

macrophages, thus disrupting the pro-tumor favoring microenvironment (X. Chauchet et al. in preparation).

The most widely used treatment for B cell lymphomas is R-CHOP (3). However, a large number of patients become refractory to rituximab with time thus representing a growing population with an unmet medical need (4). Several emerging therapies for the treatment of relapsed or refractory B cell lymphomas are in development (47), including the biAb approach presented here. A plethora of ongoing trials are evaluating the efficacy of rituximab combined with checkpoint inhibitors and other immune therapies for lymphoma (48). As such, we show that combination studies of rituximab with NI-1701 in xenograft mouse model resulted in a significantly improved tumor growth inhibition as compared to either treatment. The complementary mechanisms of action afforded by the two approaches certainly explain the significant benefit over stand-alone therapies and further investigations are ongoing to dissect mechanisms. These results also re-inforce the concept of targeting two distinct cell-surface antigens to increase the likelihood of cancer control in situations with pre-existing epitope-variants or -loss, such as reported in rituximab-refractory NHL patients (4, 49). Furthermore, NI-1701 was shown to be superior to rituximab in killing B cells from B-ALL patients and the B-ALL-derived cell line, NALM-6 cells. Data from our laboratory and others (50) have demonstrated the lower proportion of ALL patients expressing CD20 on B cell, which may explain the improved efficacy afforded by NI-1701.

The study here describes the development of a novel bispecific Ab approach harnessing macrophages through the blockade of CD47 in B cell malignancies. By targeting CD19 with high affinity, NI-1701 aims to selectively inhibit the CD47 “don’t eat me” signal on B cells. This approach offers an alternative treatment for patients resistant and/or refractory to anti-CD20 therapy. Clinical experience will validate the safe and selective strategy afforded by co-targeting CD47 and CD19 on B cells.

Acknowledgments

The authors wish to thank Dr Alison M Michie and Dr Emilio Cosimo who provided clinical samples used to establish the *in vitro* ADCP assays; Dr Stéphanie Hugues and Dr Juan Dubrot Armendariz for video microscopy; Serge Wolfersperger and Emeline Eggimann for animal husbandry.

Financial support. The R50 award (R50CA211466; NCI) supports Michael P. Rettig's research.

References

1. Smith A, Howell D, Patmore R, Jack A, Roman E. Incidence of haematological malignancy by sub-type: a report from the Haematological Malignancy Research Network. Br J Cancer 2011;105:1684-92.

2. Coiffier B. Monoclonal antibodies combined to chemotherapy for the treatment of patients with lymphoma. Blood Rev 2003;17:25-31.

3. Zelenetz AD, Abramson JS, Advani RH, Andreadis CB, Byrd JC, Czuczman MS, et al. NCCN Clinical Practice Guidelines in Oncology: non-Hodgkin's lymphomas. J Natl Compr Canc Netw 2010;8:288-334.

4. Hauptrock B, Hess G. Rituximab in the treatment of non-Hodgkin's lymphoma. Biologics 2008;2:619-33.

5. Davis TA, Czerwinski DK, Levy R. Therapy of B-cell lymphoma with anti-CD20 antibodies can result in the loss of CD20 antigen expression. Clin Cancer Res 1999;5:611-5.

6. Prevodnik VK, Lavrencak J, Horvat M, Novakovic BJ. The predictive significance of CD20 expression in B-cell lymphomas. Diagn Pathol 2011;6:33.

7. Wang K, Wei G, Liu D. CD19: a biomarker for B cell development, lymphoma diagnosis and therapy. Exp Hematol Oncol 2012;1:36.

8. Katz BZ, Herishanu Y. Therapeutic targeting of CD19 in hematological malignancies: past, present, future and beyond. Leuk Lymphoma 2014;55:999-1006.

9. Chen R, Song XT, Chen B. CD19 chimeric antigen receptor T cell therapy for the treatment of B cell lineage acute lymphoblastic leukemia. Discov Med 2015;20:185-90.

10. Portell CA, Wenzell CM, Advani AS. Clinical and pharmacologic aspects of blinatumomab in the treatment of B-cell acute lymphoblastic leukemia. Clin Pharmacol 2013;5:5-11.

11. Ramos CA, Savoldo B, Dotti G. CD19-CAR trials. Cancer J 2014;20:112-8.

12. Pardoll DM. The blockade of immune checkpoints in cancer immunotherapy. Nat Rev Cancer 2012;12:252-64.

13. Mantovani A, Allavena P. The interaction of anticancer therapies with tumor-associated macrophages. J Exp Med 2015;212:435-45.

14. Barclay AN, Van den Berg TK. The interaction between signal regulatory protein alpha (SIRPalpha) and CD47: structure, function, and therapeutic target. Annu Rev Immunol 2014;32:25-50.

15. Chao MP, Alizadeh AA, Tang C, Myklebust JH, Varghese B, Gill S, et al. Anti-CD47 antibody synergizes with rituximab to promote phagocytosis and eradicate non-Hodgkin lymphoma. Cell 2010;142:699-713.

16. Mouro-Chanteloup I, Delaunay J, Gane P, Nicolas V, Johansen M, Brown EJ, et al. Evidence that the red cell skeleton protein 4.2 interacts with the Rh membrane complex member CD47. Blood 2003;101:338-44.

17. Olsson M, Bruhns P, Frazier WA, Ravetch JV, Oldenborg PA. Platelet homeostasis is regulated by platelet expression of CD47 under normal conditions and in passive immune thrombocytopenia. Blood 2005;105:3577-82.

18. Fischer N, Elson G, Magistrelli G, Dheilly E, Fouque N, Laurendon A, et al. Exploiting light chains for the scalable generation and platform purification of native human bispecific IgG. Nat Commun 2015;6:6113.

19. Dheilly E, Moine V, Broyer L, Salgado-Pires S, Johnson Z, Papaioannou A, et al. Selective Blockade of the Ubiquitous Checkpoint Receptor CD47 Is Enabled by Dual-Targeting Bispecific Antibodies. Mol Ther 2017;25:523-33.

20. Liu J, Wang L, Zhao F, Tseng S, Narayanan C, Shura L, et al. Pre-Clinical Development of a Humanized Anti-CD47 Antibody with Anti-Cancer Therapeutic Potential. PLoS One 2015;10:e0137345.

21. Herter S, Birk MC, Klein C, Gerdes C, Umana P, Bacac M. Glycoengineering of therapeutic antibodies enhances monocyte/macrophage-mediated phagocytosis and cytotoxicity. J Immunol 2014;192:2252-60.

22. Leidi M, Gotti E, Bologna L, Miranda E, Rimoldi M, Sica A, et al. M2 macrophages phagocytose rituximab-opsonized leukemic targets more efficiently than m1 cells in vitro. J Immunol 2009;182:4415-22.

23. Mantovani A, Sica A, Sozzani S, Allavena P, Vecchi A, Locati M. The chemokine system in diverse forms of macrophage activation and polarization. Trends Immunol 2004;25:677-86.

24. Brown EJ, Frazier WA. Integrin-associated protein (CD47) and its ligands. Trends Cell Biol 2001;11:130-5.

25. Oldenborg PA. CD47: A Cell Surface Glycoprotein Which Regulates Multiple Functions of Hematopoietic Cells in Health and Disease. ISRN Hematol 2013;2013:614619.

26. Hotzel I, Theil FP, Bernstein LJ, Prabhu S, Deng R, Quintana L, et al. A strategy for risk mitigation of antibodies with fast clearance. MAbs 2012;4:753-60.

27. Ingram JR, Blomberg OS, Sockolosky JT, Ali L, Schmidt FI, Pishesha N, et al. Localized CD47 blockade enhances immunotherapy for murine melanoma. Proc Natl Acad Sci U S A 2017;114:10184-9.

28. Pietsch EC, Dong J, Cardoso R, Zhang X, Chin D, Hawkins R, et al. Anti-leukemic activity and tolerability of anti-human CD47 monoclonal antibodies. Blood Cancer J 2017;7:e536.

29. Weiskopf K, Ring AM, Ho CC, Volkmer JP, Levin AM, Volkmer AK, et al. Engineered SIRPalpha variants as immunotherapeutic adjuvants to anticancer antibodies. Science 2013;341:88-91.

30. Willingham SB, Volkmer JP, Gentles AJ, Sahoo D, Dalerba P, Mitra SS, et al. The CD47-signal regulatory protein alpha (SIRPa) interaction is a therapeutic target for human solid tumors. Proc Natl Acad Sci U S A 2012;109:6662-7.

31. King M, McDermott P, Schreiber AD. Characterization of the Fc gamma receptor on human platelets. Cell Immunol 1990;128:462-79.

32. Piccione EC, Juarez S, Liu J, Tseng S, Ryan CE, Narayanan C, et al. A bispecific antibody targeting CD47 and CD20 selectively binds and eliminates dual antigen expressing lymphoma cells. MAbs 2015;7:946-56.

33. Tedder TF, Baras A, Xiu Y. Fcgamma receptor-dependent effector mechanisms regulate CD19 and CD20 antibody immunotherapies for B lymphocyte malignancies and autoimmunity. Springer Semin Immunopathol 2006;28:351-64.

34. Beum PV, Lindorfer MA, Taylor RP. Within peripheral blood mononuclear cells, antibody-dependent cellular cytotoxicity of rituximab-opsonized Daudi cells is promoted by NK cells and inhibited by monocytes due to shaving. J Immunol 2008;181:2916-24.

35. Horton HM, Bernett MJ, Pong E, Peipp M, Karki S, Chu SY, et al. Potent in vitro and in vivo activity of an Fc-engineered anti-CD19 monoclonal antibody against lymphoma and leukemia. Cancer Res 2008;68:8049-57.

36. Kern DJ, James BR, Blackwell S, Gassner C, Klein C, Weiner GJ. GA101 induces NK-cell activation and antibody-dependent cellular cytotoxicity more effectively than rituximab when complement is present. Leuk Lymphoma 2013;54:2500-5.

37. Matlawska-Wasowska K, Ward E, Stevens S, Wang Y, Herbst R, Winter SS, et al. Macrophage and NK-mediated killing of precursor-B acute lymphoblastic leukemia cells targeted with a-fucosylated anti-CD19 humanized antibodies. Leukemia 2013;27:1263-74.

38. Ward E, Mittereder N, Kuta E, Sims GP, Bowen MA, Dall'Acqua W, et al. A glycoengineered anti-CD19 antibody with potent antibody-dependent cellular cytotoxicity activity in vitro and lymphoma growth inhibition in vivo. Br J Haematol 2011;155:426-37.

39. Greiner DL, Shultz LD, Yates J, Appel MC, Perdrizet G, Hesselton RM, et al. Improved engraftment of human spleen cells in NOD/LtSz-scid/scid mice as compared with C.B-17-scid/scid mice. Am J Pathol 1995;146:888-902.

40. Shultz LD, Schweitzer PA, Christianson SW, Gott B, Schweitzer IB, Tennent B, et al. Multiple defects in innate and adaptive immunologic function in NOD/LtSz-scid mice. J Immunol 1995;154:180-91.

41. Kwong LS, Brown MH, Barclay AN, Hatherley D. Signal-regulatory protein alpha from the NOD mouse binds human CD47 with an exceptionally high affinity-- implications for engraftment of human cells. Immunology 2014;143:61-7.

42. Chanmee T, Ontong P, Konno K, Itano N. Tumor-associated macrophages as major players in the tumor microenvironment. Cancers (Basel) 2014;6:1670-90.

43. Murray PJ, Allen JE, Biswas SK, Fisher EA, Gilroy DW, Goerdt S, et al. Macrophage activation and polarization: nomenclature and experimental guidelines. Immunity 2014;41:14-20.

44. Sica A, Mantovani A. Macrophage plasticity and polarization: in vivo veritas. J Clin Invest 2012;122:787-95.

45. Mantovani A, Marchesi F, Malesci A, Laghi L, Allavena P. Tumour-associated macrophages as treatment targets in oncology. Nat Rev Clin Oncol 2017;14:399-416.

46. Martinez FO, Gordon S. The M1 and M2 paradigm of macrophage activation: time for reassessment. F1000Prime Rep 2014;6:13.

47. MacDonald D, Prica A, Assouline S, Christofides A, Lawrence T, Sehn LH. Emerging therapies for the treatment of relapsed or refractory follicular lymphoma. Curr Oncol 2016;23:407-17.

48. Salles G, Barrett M, Foa R, Maurer J, O'Brien S, Valente N, et al. Rituximab in B-Cell Hematologic Malignancies: A Review of 20 Years of Clinical Experience. Adv Ther 2017.

49. Kennedy AD, Beum PV, Solga MD, DiLillo DJ, Lindorfer MA, Hess CE, et al. Rituximab infusion promotes rapid complement depletion and acute CD20 loss in chronic lymphocytic leukemia. J Immunol 2004;172:3280-8.

50. Ginaldi L, De MM, Matutes E, Farahat N, Morilla R, Catovsky D. Levels of expression of CD19 and CD20 in chronic B cell leukaemias. J Clin Pathol 1998;51:364-9.

Figures legends

Figure 1.

NI-1701 binds selectively to B cells. Human whole blood samples were incubated with antibodies to CD20 (for B cells), CD3 (for T cells) and CD41a (for platelets) in combination with either AF-488 labeled-isotype control Ab (grey line), AF-488 labeled NI-1701 (dark line) or AF-488 labeled anti-hCD47 mAb (hB6H12, dashed line). Erythrocytes were gated based on SSC/FSC parameters. Samples were analyzed by flow cytometry.

Figure 2.

Blockade of CD47/SIRPα enhances phagocytosis of tumor B cells. **A,** Percentage of phagocytosis by macrophages of CFSE-labeled Raji cells after treatment with 10 μg/mL of hIgG1 control, or a dose-range of NI-1701, the CD47 monovalent Ab, the CD19 monovalent Ab and the CD19 bivalent Ab. **B,** The number of CD19, CD20 and CD47 per cell on Raji cells or the CD47-silenced clone Raji cells was quantified using the Qifikit®. Histograms represent the mean $\pm$ SD of 3 experiments. The mean is indicated above the histograms. **C**, Percentage of phagocytosis by macrophages of CFSE-labeled Raji cells or CFSE-labeled CD47 silenced Raji cells after treatment with a dose-range of rituximab. **D**, Percentage of phagocytosis by macrophages of CFSE-labeled Raji cells or CFSE-labeled CD47-silenced Raji cells after treatment with a dose-range of NI-1701 or the monovalent CD19 Ab. **A, C, and D**, Data were obtained by flow cytometry; percentage of phagocytosis is expressed as the percentage of CFSE/CD14 double positive events among $CD14^+$ macrophage cells. Graphs depict a representative dose response curve of a minimum of 3 independent experiments.

Figure 3.

NI-1701 mediates killing of B lymphoma and leukemic cell lines by different subtypes of macrophages or killing by IL-2 stimulated PBMCs by ADCC. **A**, Phagocytosis of CFSE-labeled Raji, Ramos, NALM-6, MEC-2 and SUDHL-4 cells by macrophages after treatment with 10 μg/mL of hIgG1 control Ab, NI-1701 or rituximab. Phagocytosis was assessed by flow cytometry and expressed as a percentage of CFSE/CD14 double positive events among $CD14^+$ macrophages cells. Histograms

are representative of 2 to 6 independent experiments, depending on the cell lines. **B,** Phagocytosis of CFSE-labeled Raji by macrophages differentiated into M0, M1, M2a or M2c subset after treatment with 10µg/mL of hIgG1 control or NI-1701. A minimum of 13 donors were used to differentiate macrophage subtypes and each point represent one unique donor. Phagocytosis was assessed as above. Statistical analysis was performed using the paired Student T test. ***p<0.001. **C**, Cr51-labelled Raji cells were incubated with a fixed concentration of hIgG1 control Ab (1µg/mL), or a dose-range of NI-1701 (15 min, RT). These cells were then incubated (4h, 37°C) in the presence of IL2-stimulated PBMC as a source of effector cells (E:T 80:1). The graph depicts the % of specific ADCC with the mean ± SD. Graphs depict a representative dose response curve of minimum 5 independent experiments.

Figure 4.

NI- 1701 controls tumor growth in a subcutaneous xenograft model and synergizes with rituximab. **A**, NOD/SCID mice were subcutaneously (s.c.) injected with $5x10^6$ Raji cells. When tumors reached a volume of 100 mm^3, mice were randomized into the following treatment groups: hIgG1 control (n=8); NI-1701 (n=8); CD19 monovalent Ab (n=8), CD47 monovalent Ab (n=8) or CD19 bivalent Ab (n=7). Abs were injected i.v. at 20 mg/kg, once a week (days 0, 7, 14 and 21). (**A, upper panel**), The mean tumor volume (± SEM) per group is depicted over time. Statistical analyses were performed on the calculated area under the curve using a one-way ANOVA followed by a Tukey's multiple comparison test. *p<0.05;**p<0.01;****p<0.0001. (**A, lower panel**), Tumor growth was monitored beyond the end of the treatment period until day 39. Mice were euthanized when the endpoint was reached (tumor volume≈1400 mm^3) or at the end of the study (day 39). For comparison of survival curves (Kaplan Meier curves), a log-rank (Mantel-Cox) test was performed. p< 0.05 is considered to be statistically significant. **B,** NOD/SCID mice were subcutaneously (s.c.) injected with $5x10^6$ Raji cells. When tumors reached a volume of 100 mm^3, mice were randomized into the following treatment groups: hIgG1 control (n=8); NI-1701 (n=8); rituximab (n=8) or the combination of NI-1701 + rituximab (n=8). Abs were injected i.v. at 20 mg/kg for single treatment or 10mg/kg + 10mg/kg for combination, once a week (days 0, 7, 14 and 21). (**B, upper panel**), The mean tumor volume (± SEM) per group is depicted over time. Statistical analyses were performed on the calculated area under the curve using a one-way ANOVA followed by a Tukey's multiple comparison test. *p<0.05;**p<0.01;****p<0.0001. (**B, lower panel**), Tumor growth was monitored beyond the end of the treatment period until day 60. Mice were euthanized when the endpoint was reached (tumor volume ≈ 1400mm^3) or at the end of the

study (day 60). For comparison of survival curves (Kaplan Meier curves), a log-rank (Mantel-Cox) test was performed. $p< 0.05$ is considered to be statistically significant.

Figure 5.

Non-human primate studies demonstrate favorable pharmacokinetics and normal hematological parameters of NI-1701 following one single injection or multiple weekly injections. **A-C,** NI-1701 and/or CD19/CD47^{hi} were administered to cynomolgus monkeys as a single intravenous bolus at 0.5 or 10mg/kg (n=3 animals per treatment group per dose group). An ELISA assay was developed in-house to measure NI-1701 or CD19/CD47^{hi} biAb serum concentration. (**A**), The elimination profile of NI-1701 at both doses are shown. The horizontal dotted line represents the lower limit of quantification (LLOQ) of the ELISA assay. (**B**), The distribution phase (up to 24h) of the PK profiles of NI-1701 and CD19/CD47^{hi} at high doses (10 mg/kg, left hand panel) and at low doses (0.5 mg/kg, right hand panel) are compared. (**C**), IL-6 serum concentrations were quantified for NI-1701 and/or CD19/CD47^{hi} treated animals for the dose at 10mg/kg. Statistical analysis was performed using Mann-Whitney test. ***$p<0.001$. **D and E,** A DRF study was conducted. Cynomolgus monkeys (2 females and 1 male per group) were administered weekly i.v. bolus doses of vehicle or NI-1701. Treated animals received two escalating doses of NI-1701: 2 injections at 30 mg/kg (days 1 and 8) followed by 2 injections at 100 mg/kg (days 15 and 22). (**D**), The elimination profile of NI-1701 following 2 injections at 30 mg/kg and 2 injections of 100 mg/kg is shown. (**E**), Hematological parameters were monitored predose and over 4 weeks of dosing; red blood cell and platelet counts are shown. The horizontal dotted lines indicate the normal reference values for this species.

Figure 6.

NI-1701 mediates effective killing of B cells from a range of primary human samples *in vitro* and *in vivo*. **A,** Percentage of phagocytosis by macrophages of CFSE-labeled primary samples from 24 CLL patients, 15 ALL patients and 12 NHL patients including 3 MZL, 2 WM, 3 MCL, 4 FL and 1 DLBCL. Primary samples were treated with 10μg/ml of hIgG1 control, NI-1701 or rituximab (RTX). Phagocytosis % was assessed by flow cytometry and expressed as the percentage of CFSE/CD14 double positive events among CD14^{+} macrophages cells. Each symbol corresponds to one sample, the lines represent the mean of phagocytosis % $\pm$ SEM. **B**, Examples of FlowSight® acquisitions showing target cells (stained with CFSE, green fluorescence, Ch02) and macrophage (stained with CD14-APC,

red fluorescence, Ch11). Ch05 corresponds to the IDEAS software quantification counting the number of B-CLL cells inside macrophages. Ch02/Ch11 corresponds to the merged acquisition between Ch02 and Ch11. Row 1 is representative picture of empty macrophages. Row 2 demonstrated the specific counting of engulfed target cells versus non-engulfed ones. Rows 3 and 4 show representative pictures of macrophages with several engulfed target cells. Graph represents the phagocytosis index for hIgG1 control Ab, NI-1701 and rituximab (RTX) treated B-CLL primary samples (n=14) tested at 10 μg/mL. Each symbol corresponds to one sample, the lines represent the mean of phagocytosis % ± SEM. **C**, Percentage of phagocytosis by M2 macrophages of pH-rodo-labeled purified B cells from 10 FL primary samples and treated with 10μg/mL of hIgG1 control, NI-1701 or rituximab (RTX). Phagocytosis % was assessed by fluorescent microscopy with the acquisition of 100 macrophages. Each symbol corresponds to one sample, the lines represent the mean of phagocytosis % ± SEM. **D**, NSG mice irradiated 2 days earlier (275cGy) were injected i.v. with 1.8 x 10^6 PBMC from an ALL patient. 7 days later, the first dose of hIgG1 control (n=5) or NI-1701 (n=8) was administered i.v. (20 mg/kg). Dosing has continued once a week throughout the study which was terminated at day 38. The absolute number of B-ALL tumor cells following flow cytometry acquisition (based on $hCD45^+$ staining) in one femur for the BM, PB (per μL), spleen and liver from mice treated with NI-1701 or hIgG1 isotype control are depicted. Each dot represents an individual mouse and the horizontal bar the mean ± SD. Statistical analyses were performed using paired One-Way ANOVA followed by multiple comparison tests (A, B and C) or unpaired t test (D). **p<0.01, ***p<0.001 and ****p<0.0001.

Figure 1.

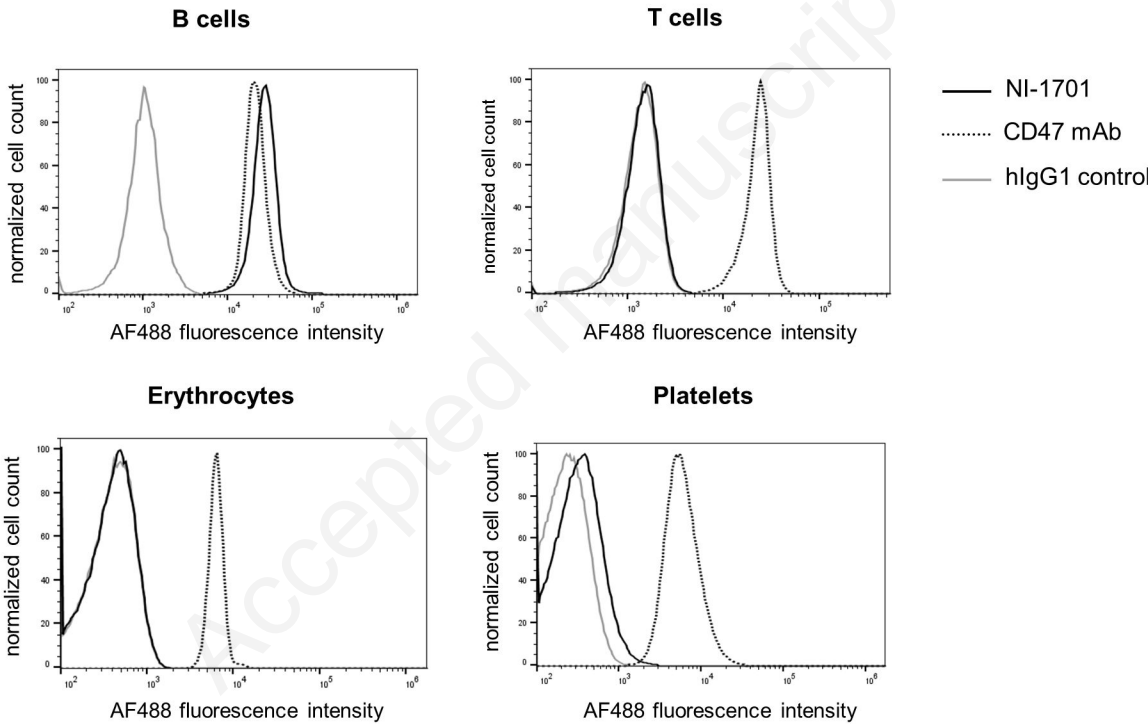

Figure 2.

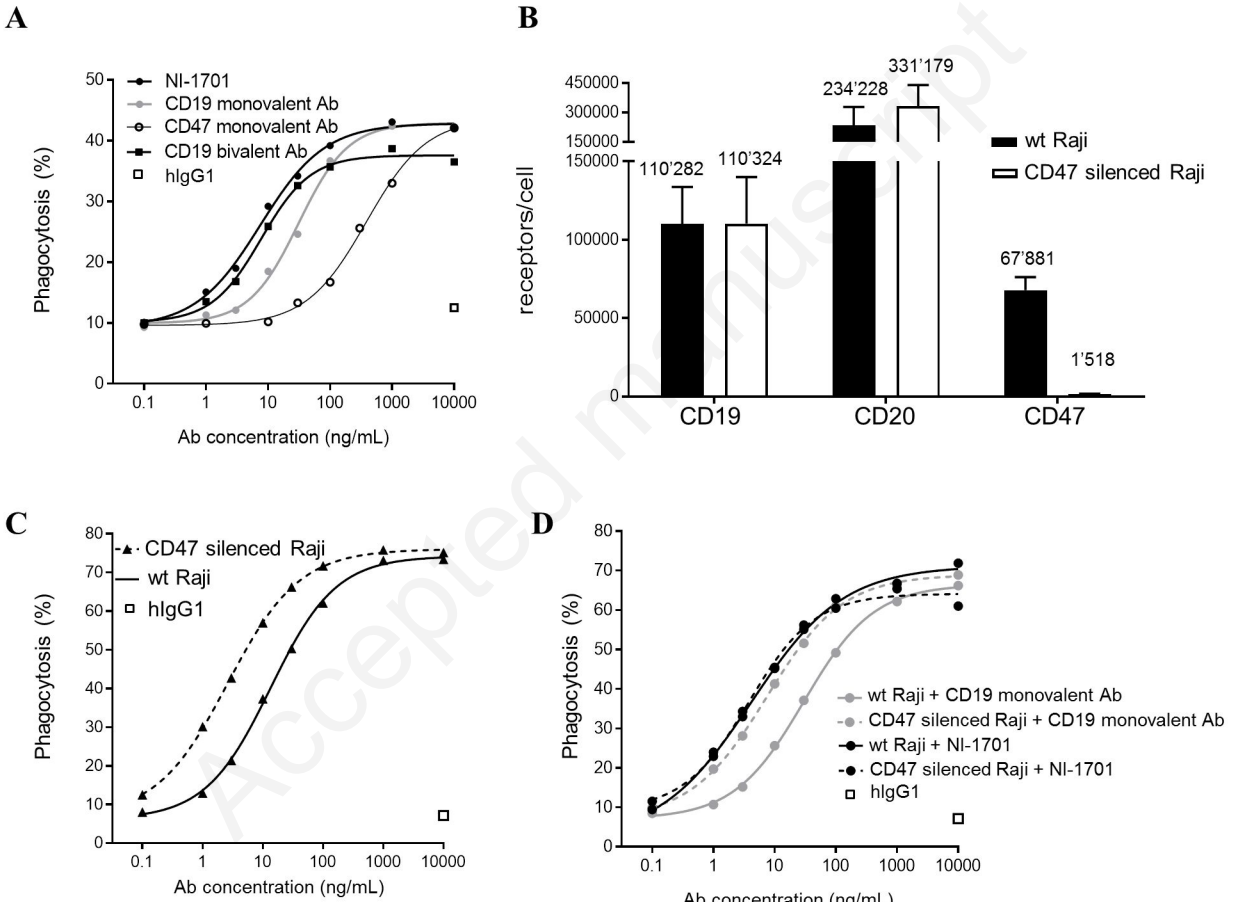

Figure 3.

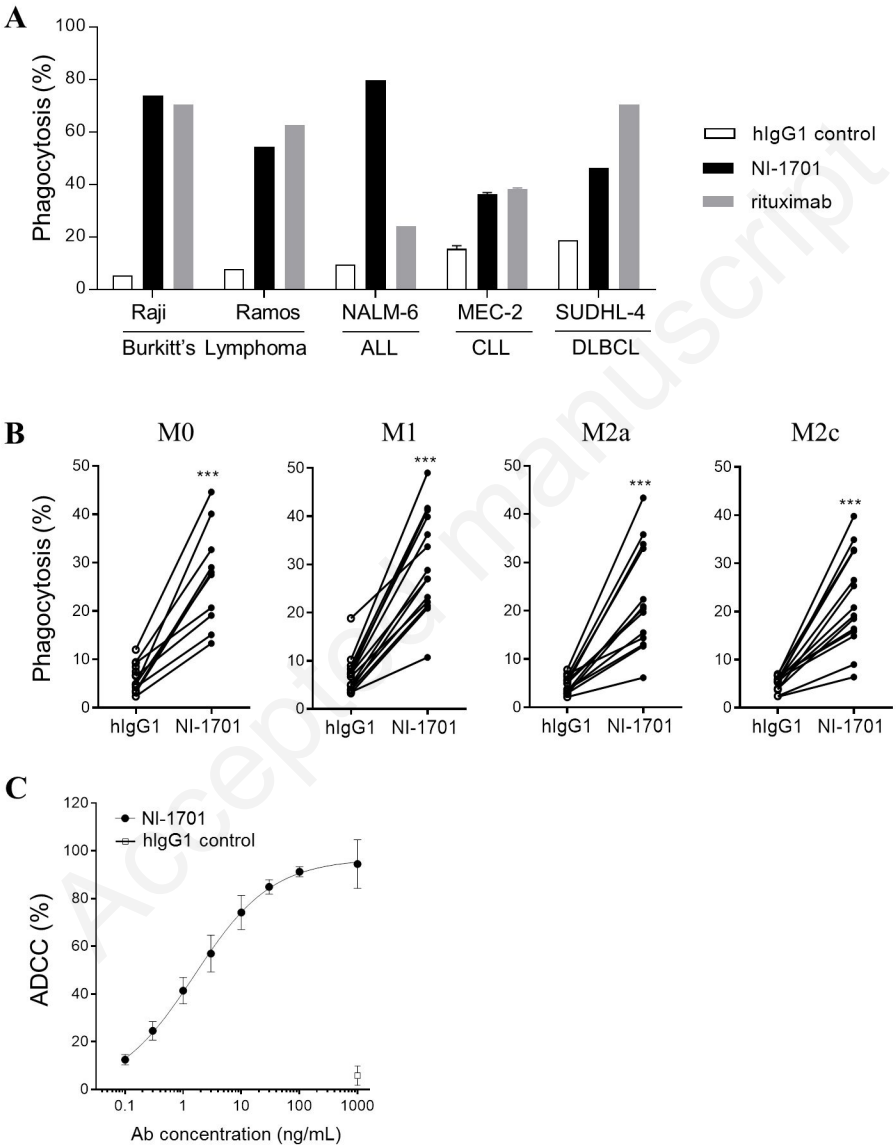

Figure 4.

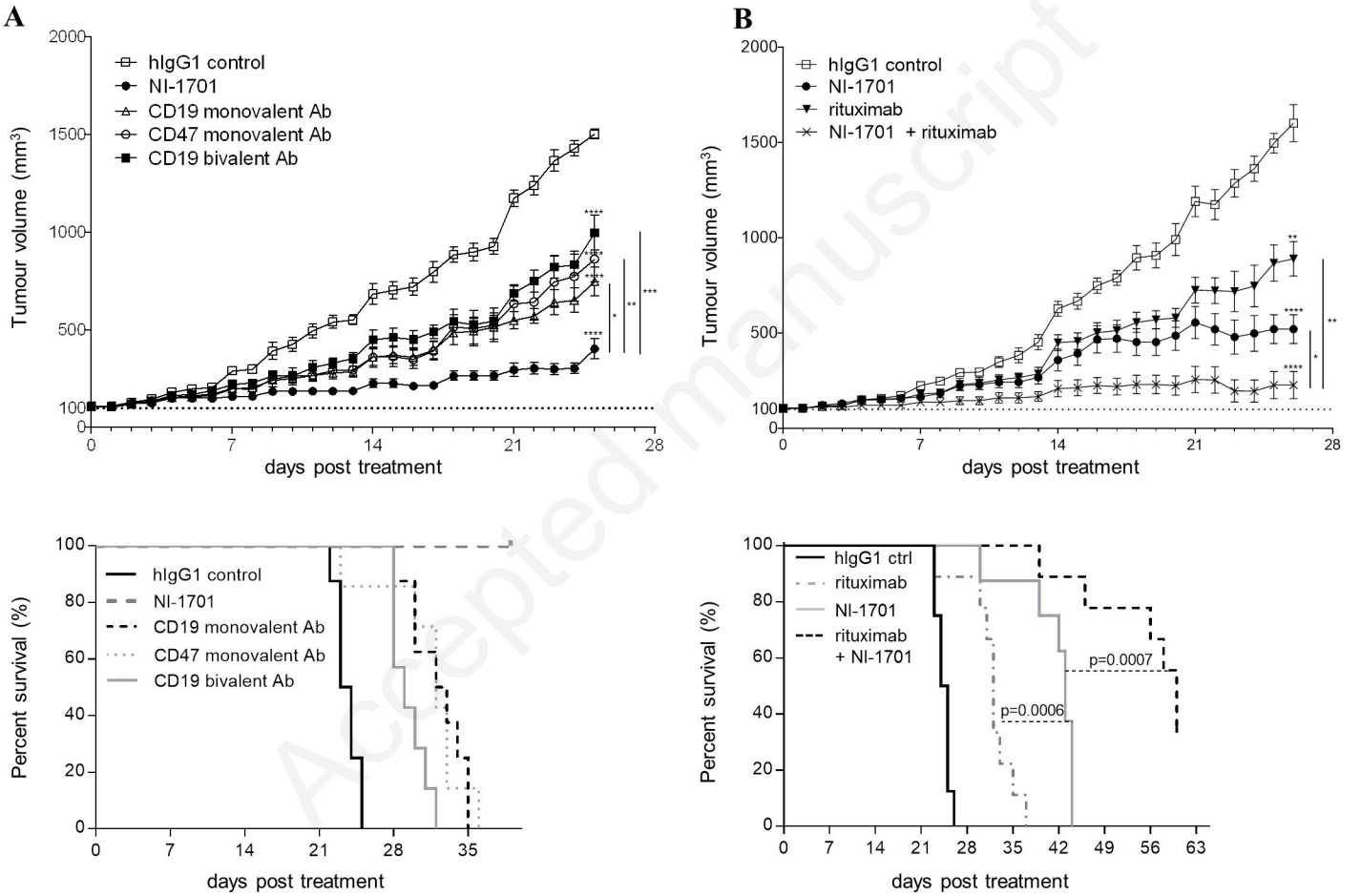

Figure 5.

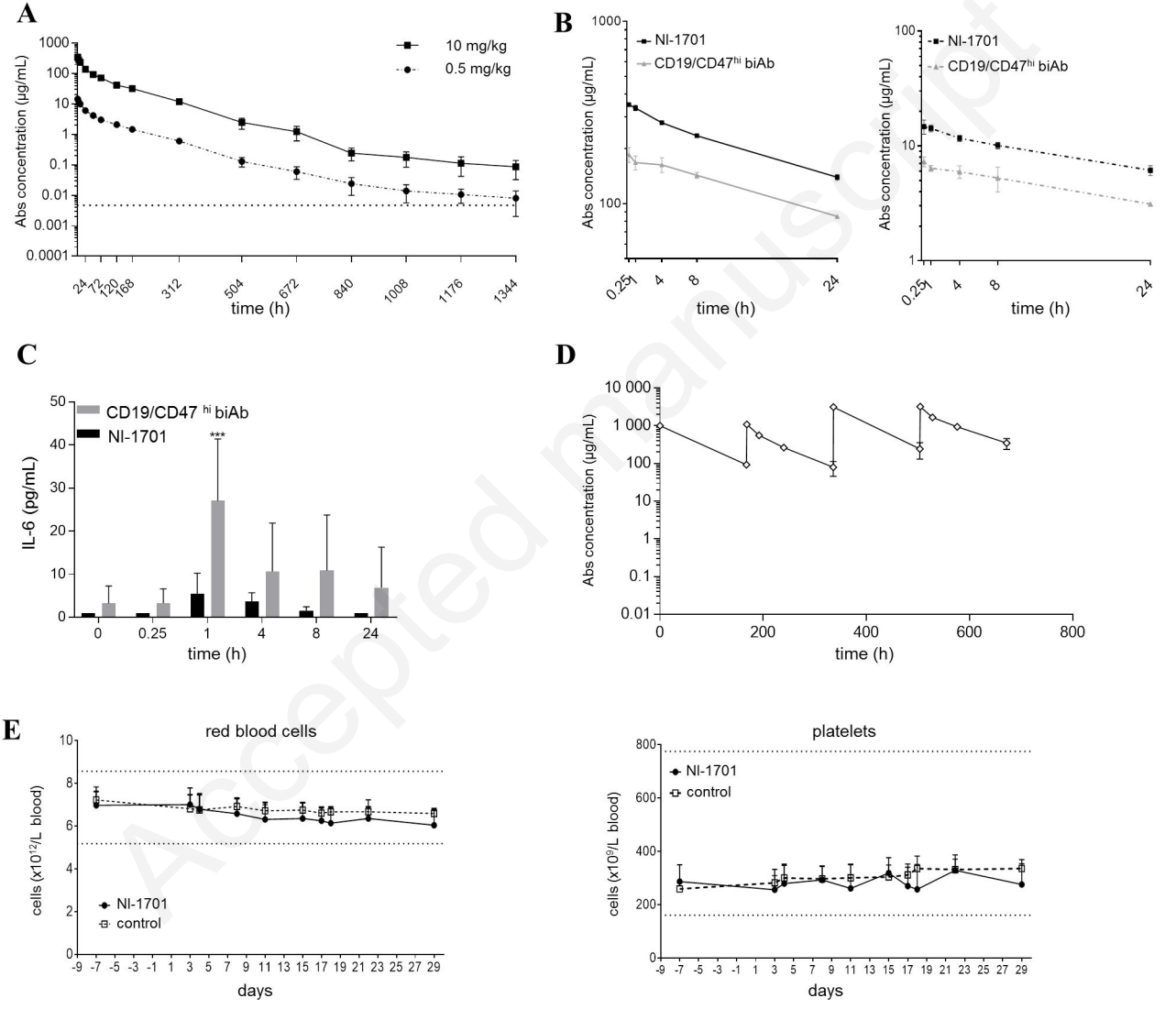

Figure 6.